Arch. Metall. Mater. **69** (2024), 2, 485-488

DOI: https://doi.org/10.24425/amm.2024.149772

YOUNG-CHUL SHIN[1], SEONG-HO HA[1*]

TEM INVESTIGATION ON MICROSTRUCTURES OF AGE-HARDENED 2014 Al ALLOY FORGED BY COLD BIAXIAL ALTERNATE FORGING

In this study, microstructures of age-hardened 2014 Al alloy forged by cold biaxial alternate forging was investigated by transmission electron microscope. And also, the forming limits of age-hardened 2014 Al alloy were examined using both conventional compression test and biaxial alternate forging. As a result of compression test, it showed a perfect plastic behavior with no visible change in stress after 27% in strain and eventually, the curve fluctuated as a shear crack occurs after 51% strain. However, it was possible to impose very large strains on the 2014-T6 Al alloy workpieces through the biaxial alternate forging of up to 4 passes. The effective strain was possibly accumulated to 356% and 204% as the maximum and average values, respectively. The results of transmission electron microscope indicated that the high density dislocations were distributed after 3 passes. After 4 passes, the distribution of more increased dislocations was observed and band-shaped dislocation clustering appeared.

Keywords: Biaxial alternate forging; Severe plastic deformation; 2014 Al alloy; Precipitation; Transmission electron microscope

1. Introduction

The forgeability of a metallic material can be explained as its capability to undergo deformation by forging without cracking. A number of forgeability tests have been developed to measure forgeability. One of the commonly used tests is the upsetting test, which simulate the forming characteristics during upsetting process. In the previous study, the forgeability of Al wrought alloys was examined by a biaxial alternate forging using the upsetting system self-developed [1]. Al-Mg based alloys, one of the non-heat treatable Al alloys, were mainly subjected to the test. It was also found that a significant amount of strain was accumulated even under cold forming condition. This study focuses on whether it is possible to apply large amounts of strain to age-hardening Al alloys through the upsetting test mentioned above.

2xxx series Al-Cu alloys are widely used in aircraft industry where their high strength is required [2]. Among 2xxx series, AA2024, the most popular Al-Cu alloys, has recently been replaced with AA2014. AA2014 is an Al-Cu-Mg based alloy which is a promising candidate in the high specific strength structural materials [2]. Various studies on severe plastic deformation (SPD) behaviors of 2xxx series alloys have been reported [3-5]. Wang et al. [3] investigated the grain structures of 2014 Al alloy at different cumulative strain after multidirectional forging at 350 ℃. Prakash et al. [6] studied the tensile, compressive and flexural behaviours of 2014-T6 Al alloy at different strain rates and temperatures including room temperature. However, few researches have been concerned about cold SPD behavior of 2xxx Al alloys. It was judged that it is possible to apply a large amount of strain to the 2xxx series alloys when using the above mentioned biaxial alternate forging. In addition, when SPD was applied to an age-hardened alloy, it was thought possible to observe the response of precipitates to SPD. In this study, microstructures of age-hardened 2014 Al alloy forged by cold biaxial alternate forging was investigated by transmission electron microscope (TEM). And also, the forming limits of age-hardened 2014 Al alloy were examined using both conventional compression test and biaxial alternate forging.

2. Experimental

The experimental material examined in this study is an extruded 2014 Al alloy billet (provided by domestic Al alloy manufacturer) whose nominal composition is given elsewhere [2]. The extruded 2014 Al alloy was subjected to T6 heat treatment [2]. The sample was solution heat treated at 500°C

[1] KOREA INSTITUTE OF INDUSTRIAL TECHNOLOGY (KITECH), INCHEON 21999, REPUBLIC OF KOREA

* Corresponding author: seonghoha1999@gmail.com

for 5 hours and water quenched, followed by artificial aging at 180°C for 9.5 hours. Compression and tensile tests on 2014-T6 Al alloy were carried out. Tensile test specimen was machined according to ASTM: B557M-10 standards. The compression test was performed at a strain rate of 0.005/s for cylindrical specimens with a diameter of 12 mm and a height of 18 mm. Details of biaxial alternate forging test conducted for SPD are given in Fig. 1. The 2014-T6 Al alloy workpiece was rotated by 90° along its longitudinal axes for each forging pass as shown in Fig. 1(a). Fig. 1(b) displays a rod-shaped workpiece (∅19×108 mm) with octangular rod-shaped dies for the repetitive compression. The die cavity shape and the dimension of a fully deformed workpiece, respectively, are also shown in Fig. 1(c) and 1(d). The round shape of both ends in the die cavity and workpiece restricted the strain along the longitudinal direction as can be seen in Fig. 1(b) and 1(c). The test was conducted at room temperature (cold) using a hydraulic press with a capacity of 150 tons.

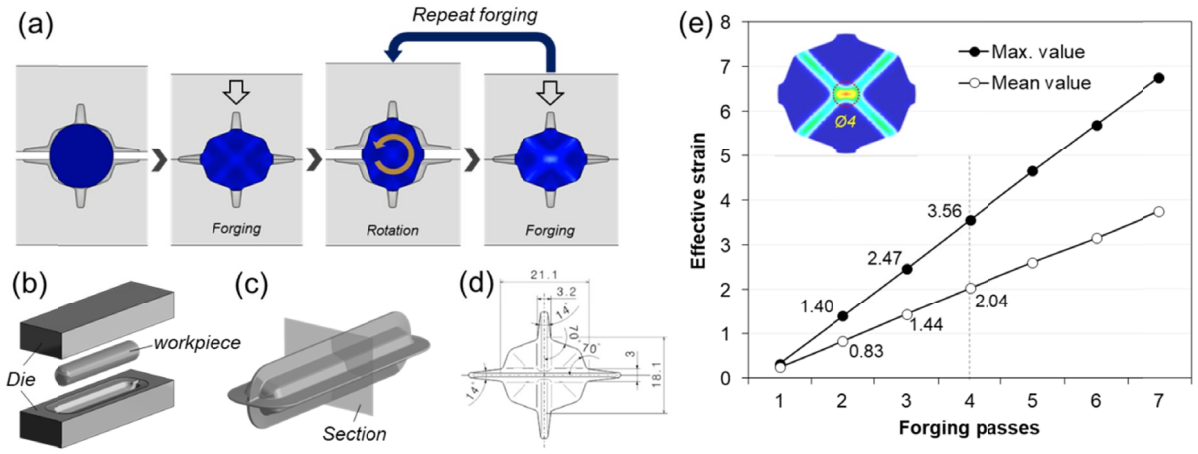

Fig. 1. Schematic 3D views of (a) biaxial alternate forging process, (b) dies and workpiece, (c) die cavity shape, (d) dimensions of section and (e) accumulated effective strain on workpiece depending on the number of forging passes

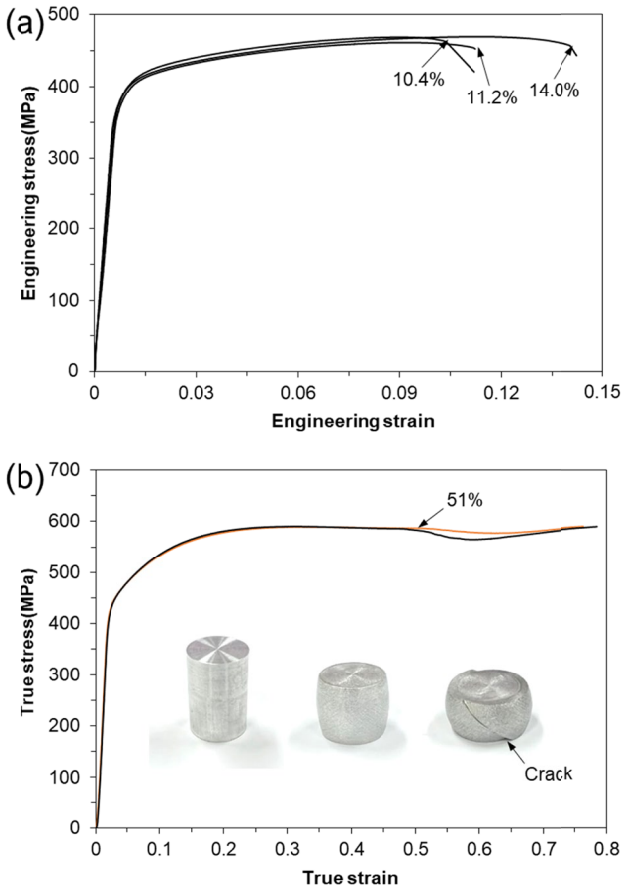

Fig. 2. (a) Tensile stress-strain curves and (b) compressive stress-strain curves of 2014-T6 Al alloy obtained at room temperature

The distribution of precipitates and dislocation in the as-forged samples were observed using a 200-kV field-emission transmission electron microscope (JEOL-2100F, JEOL, Japan) equipped with an energy-dispersive X-ray spectroscopy (EDS) detector. The TEM specimens were prepared as 3-mm-diameter, 100-mm-thick disk-type plates via mechanical polishing with a digitally enhanced precision specimen grinder (DEPS-101). Before being inserted into the TEM chamber, the specimens were trimmed and cleaned by precision ion polishing with a 691 PIPS device (Gatan) and subjected to plasma cleaning with a Fischione 1020 cleaner.

3. Results and discussion

Fig. 2 presents tensile stress-strain curves and compressive stress-strain curve of 2014-T6 aluminum alloy obtained at room temperature. Average values of ultimate tensile strength and fracture strain corresponded to about 467 MPa and 11.9%, respectively. According to a previous study reported by Prakash et al. [6], the 2014-T6 Al alloy was sensitive to increasing strain rate in tensile test. It showed higher ductility at low strain rates compared to that at high strain rates. Therefore, the tensile test values may differ from those of other literatures depending on the test conditions as well as the heat treatment conditions. As a result of compression test, it shows a perfect plastic behavior with no visible change in stress after 27% in strain. Eventually, the curve fluctuates as a shear crack occurs after

51% strain. Based on the result in the current test, it is confirmed that a deformation method such as biaxial alternate forging test aforementioned which can delay cracking is needed in order to realize a SPD with a strain of more than 50% on the 2014-T6 Al alloy. In this study, it was possible to impose very large strains on the 2014-T6 Al alloy workpieces through the biaxial alternate forging of up to 4 passes. As shown in Fig. 1, accumulated effective strain on workpiece depending on the number of forging passes simulated finite element analysis (FEA) software DEFORM 3D is shown in Fig. 1(e). The maximum and mean values of effective strain amount concentrated in the core (the area of 4 mm in diameter) increase significantly depending on the pass number. And also, it can be seen that the effective strain can be accumulated to 356% and 204% as the maximum and average values, respectively, with increasing the pass number up to 4.

TABLE 1

Analyzed compositions of areas indicated in Fig. 3 by STEM-EDS

Area	Analyzed composition (at%)					
	Al	Cu	Mg	Si	Mn	Fe
1	98.29	1.32	0.16	0.04	0.08	0.04
2	96.82	2.12	0.61	0.27	0.03	0.07
3	96.40	2.39	0.69	0.36	0.12	0.03

Fig. 3 shows the TEM images and diffraction spots on the precipitates distributed in the 2014-T6 Al alloy. The needle-like and dot-like precipitates are found in the bright-field TEM images. The two precipitates were identified as Q' and θ', respectively, which are in good agreement with those in a previous study [7]. Fig. 4 shows the bright-field and dark-field TEM images on the matrix in the 2014-T6 Al alloy after 3 passes. The distribution of high density dislocations was observed. And also, dislocation tangles were locally found. After 4 passes, the distribution of more increased dislocations was observed and band-shaped dislocation clustering appeared as shown in Fig. 5. From the above results, it was confirmed that it was possible to observe the dislocation behavior by imposing very large trains to high-strength heat-treated alloys such as 2014 Al alloy using the SPD technique self-developed and taking samples from the core where the strain was concentrated.

4. Conclusions

From the compression test, it was confirmed that the strain limit of 2014-T6 Al alloy was approximately 51% as the stress-strain curve fluctuated as a shear crack occured after 51% strain. On the other hand, it was possible to impose very large strains up to 356% and 204% as the maximum and average values, respectively, on the core of 2014-T6 Al alloy workpieces through the biaxial alternate forging of up to 4 passes. The TEM results indicated that the high density dislocations were distributed after 3 passes. After 4 passes, the distribution of more increased dislocations was observed and band-shaped dislocation clustering appeared. From the results in this study, it was considered that it was possible to observe the dislocation behavior by imposing very large trains to high-strength heat-treated alloys such as 2014 Al alloy using the SPD technique self-developed and taking samples from the core where the strain was concentrated.

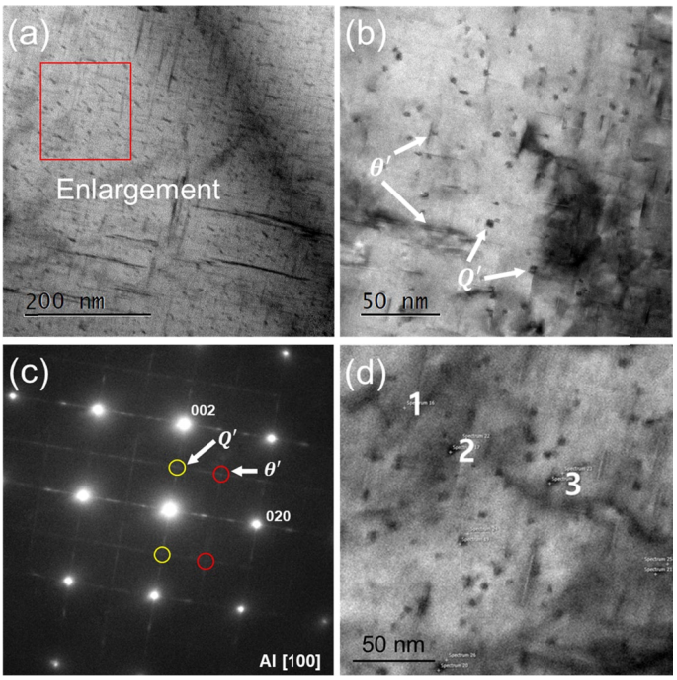

Fig. 3. (a) Bright-field TEM image of analyzed area, (b) enlargement of the analyzed area, (c) selected area diffraction pattern of Fig. 3 (b), and (d) areas analyzed by STEM-EDS

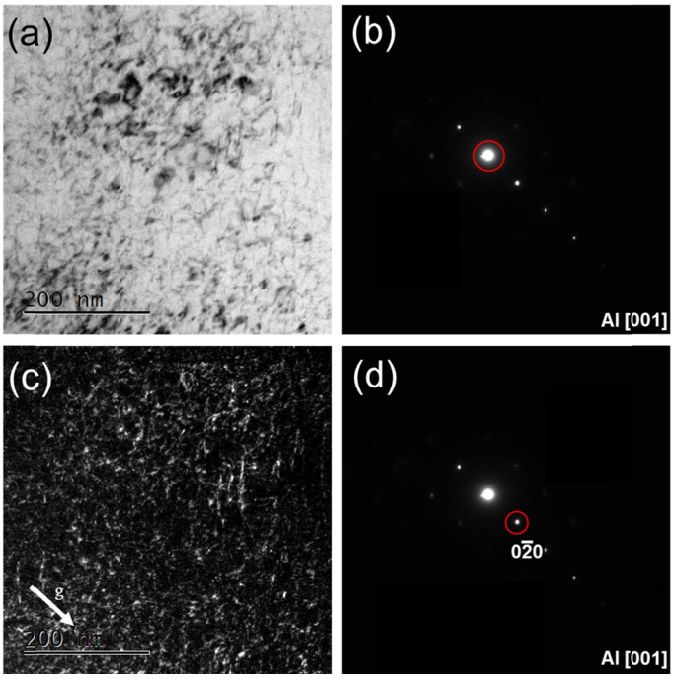

Fig. 4. (a) Bright-field TEM image of analyzed area, (b) corresponding selected area diffraction pattern, (c) dark-field TEM image, and (d) corresponding selected area diffraction pattern after 3 pass

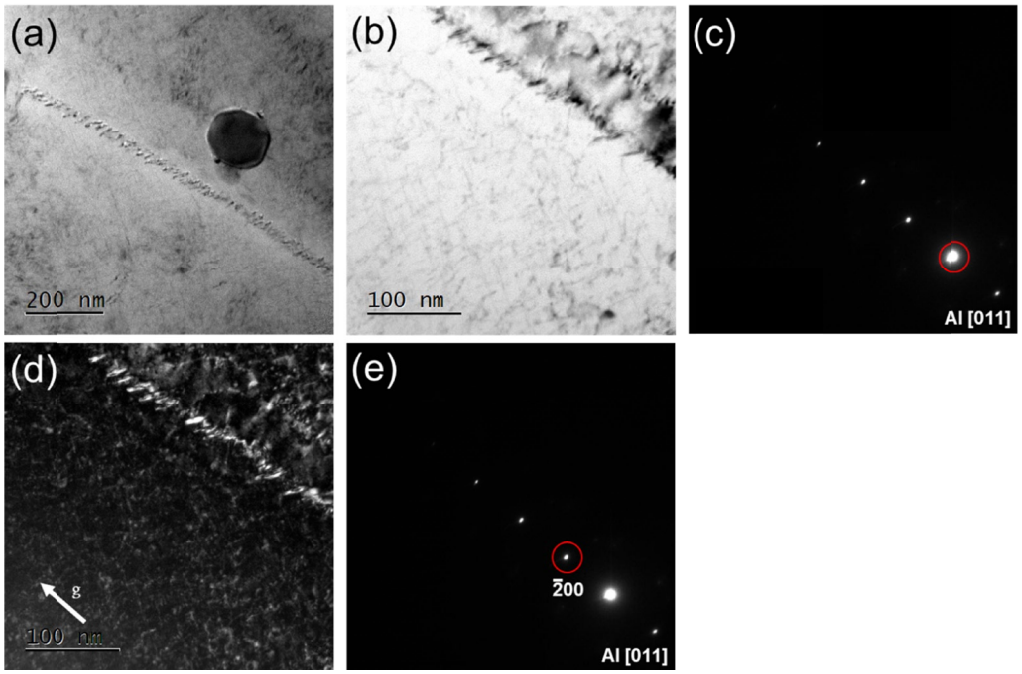

Fig. 5. (a) Bright-field TEM image of analyzed area, (b) enlargement of (a), (c) corresponding selected area diffraction pattern, (d) dark-field TEM image, and (e) corresponding selected area diffraction pattern after 4 pass

Acknowledgments

This study has been conducted with the support of the Ministry of Trade, Industry and Energy as "Materials/Parts Technology Development Program (20011420)".

REFERENCES

[1] Y.C. Shin, S.H. Ha, B.H. Kim, Y.O. Yoon, S.H. Lim, H.J. Choi, S.K. Kim, S.K. Hyun, J. Mater. Process. Technol. **286**, 116822 (2020).

[2] J.R. Davis, ASM International, Aluminum and Aluminum Alloys, Materials Park 1993.

[3] M. Wang, L. Huang, W. Liu, Mater. Sci. Eng. A **674**, 40 (2016).

[4] I. Mazurina, T. Sakai, H. Miura, Mater. Sci. Eng. A **486**, 662 (2008).

[5] H. He, Y. Yi, S. Huang, Y. Zhang, Mater. Sci. Eng. A **712**, 414 (2018).

[6] G. Prakash, N.K. Singh, N.K. Gupta, Structures **26**, 193 (2020).

[7] S. Chen, F. Li, K. Chen, L. Huang, G. Peng, Mater. Charact. **167**, 110510 (2020).